

Observation of Modulational Instability in Nd-Laser Beat-Wave Experiments

F. Amiranoff,⁽¹⁾ M. Laberge,⁽¹⁾ J. R. Marquès,⁽¹⁾ F. Moulin,⁽¹⁾ E. Fabre,⁽¹⁾ B. Cros,⁽²⁾
G. Matthieussent,⁽²⁾ P. Benkheiri,⁽³⁾ F. Jacquet,⁽³⁾ J. Meyer,⁽³⁾ Ph. Miné,⁽³⁾ C. Stenz,⁽⁴⁾ and P. Mora⁽⁵⁾

⁽¹⁾Laboratoire d'Utilisation des Lasers Intenses, Ecole Polytechnique, 91128 Palaiseau, France

⁽²⁾Laboratoire de Physique des Gaz et des Plasmas, Université Paris Sud, 91405 Orsay, France

⁽³⁾Laboratoire de Physique Nucléaire des Hautes Energies, Ecole Polytechnique, 91128 Palaiseau, France

⁽⁴⁾Groupe de Recherche sur l'Energétique des Milieux Ionisés, Université d'Orléans, 45000 Orléans, France

⁽⁵⁾Centre de Physique Théorique, Ecole Polytechnique, 91128 Palaiseau, France

(Received 13 December 1991)

The modulational instability of the high-phase-velocity plasma wave generated by a Nd-laser beat wave has been observed for the first time. Both ion and electron waves are detected when the electron density is close to the resonant density for which the plasma frequency is equal to the difference frequency between the two pump lasers. We also detect the presence of harmonics of the beat frequency which are a signature of high-amplitude density perturbations.

PACS numbers: 52.40.Nk, 52.35.Fp, 52.35.Mw, 52.75.Di

The need for new particle acceleration techniques has led to a number of works on the possibility of using plasmas to convert the transverse electric field of a high-power laser into a high-amplitude high-phase-velocity electrostatic field. Plasmas can sustain electric fields many orders of magnitude higher than available in conventional accelerating structures [1]. Presently most of the experimental work has been done on the beat-wave concept. A relativistic electron plasma wave is excited by the beating of two copropagating intense laser beams with slightly different frequencies. This is a resonant process in which the natural oscillation frequency of the electrons ω_p has to be close to the difference frequency $\delta\omega$ between the two lasers. The wave amplitude grows in time until it saturates because of different possible mechanisms [2,3]. The relativistic plasma wave has been observed in CO₂ ($\lambda \approx 10 \mu\text{m}$) laser beat-wave experiments [4-8] and its saturation attributed to relativistic detuning [7] or mode coupling with the ion waves generated by stimulated Brillouin scattering [5]. The beat wave has also been observed with Nd ($\lambda \approx 1 \mu\text{m}$) lasers [9]. In these experiments, we produce electron plasma waves by the beat-wave method using two 1- μm laser beams. These electron waves then decay by modulational instability (MI) [3] into ion waves and electron waves of lower phase velocities, which we then detect. MI is a four-wave coupling: A high-amplitude electron plasma wave decays into ion density perturbations and two daughter electron waves. The maximum coupling is obtained for daughter waves along the plasma-wave electric field, but taking into account a possible finite aperture for the original plasma waves, we can expect daughter waves in all directions.

The experimental setup is shown in Fig. 1. The two pulses delivered by a Nd-YAG and a Nd-YLF oscillator are amplified in the laser chain of LULI up to 7 J with an output diameter of 90 mm. The YAG (YLF) pulse at 1.064 μm (1.053 μm) wavelength is 160 ± 10 ps (90 ± 10 ps) wide (FWHM). A 30-mm-diam KDP frequency-doubling crystal set up in the middle of the main beam

generates a 300-mJ green ($\lambda = 5320 \text{ \AA}$) probe beam. A 1-m-focal-length bichromatic doublet focuses these beams in the middle of the gas chamber filled with deuterium. A 30-mm-diam block is put at the center of the YLF beam in order to avoid any wave coupling and satellite generation in the optical elements traversed by the three beams of different wavelengths [10]. The focal spots are imaged with a high magnification on a charge-coupled-device camera giving diameters of $100 \pm 20 \mu\text{m}$ (FWHM) and $40 \pm 10 \mu\text{m}$ for the infrared and green beams, respectively. The maximum intensities of the pump beams are $3.2 \times 10^{14} \text{ W/cm}^2$ (YAG) and $6 \times 10^{14} \text{ W/cm}^2$ (YLF). The pressure and temperature of the gas are adjusted with an accuracy that allows a precision on the initial atomic density better than 0.3%. Preceding experiments [11-13] have shown that near the focus of the lens the gas is fully ionized by multiphoton ionization so that the initial electron density is equal to the atomic density. The probe beam light scattered in the plasma is im-

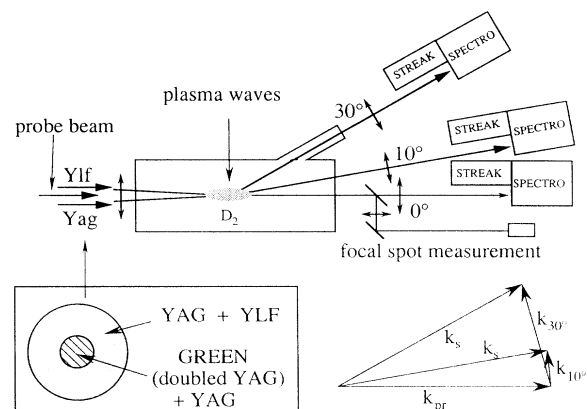


FIG. 1. Experimental setup. The three wavelengths (YAG, YLF, and doubled YAG) are spatially distributed as shown and focused in the middle of the gas chamber. k_{pr} , k_{10° , and k_{30° are the wave vectors of the probe beam and those measured at 10° and 30°. k_{0° is on the axis and $\approx k_{pr}/191$.

aged with a magnification of 1 at the entrance of two spectrograph-streak-camera combinations at two different angles: 0° ($f/30$ optics) and 10° or 10° and 30° ($f/10$). The gas chamber and the alignment system are described in detail in Ref. [12].

The on-axis relativistic plasma wave generated by the beat wave can only be detected on the 0° channel. Nevertheless, taking into account the aperture of the focusing lens ($f/11$), the beat wave may generate plasma waves, of wave vector $\mathbf{k}_{\text{YLF}} - \mathbf{k}_{\text{YAG}}$, inside a cone centered on the laser axis with a half-angle of 83° . The MI then generates a broad spectrum of waves. The 10° and 30° channels detect instability waves propagating at nearly 90° with respect to the laser axis. From the measured electron temperature [13] ≈ 15 eV and density $\approx 10^{17}$ cm^{-3} , we infer a Debye length λ_D of $0.1 \mu\text{m}$. Then for 0° , 10° , and 30° the wave vectors correspond to $k\lambda_D = 0.005, 0.18,$ and 0.55 and the phase velocities v_ϕ of the waves with frequency $\delta\omega$ correspond to $v_\phi/c \approx 1, 0.03,$ and 0.01 , respectively.

A typical time-resolved spectrum obtained on the 10° channel near the resonant density is shown in Fig. 2. The central unshifted line is attributed to ion waves with very low frequencies. On each side of this central line appear two or three satellites with frequency shifts equal to $\delta\omega$, $2\delta\omega$, and $3\delta\omega$. Figures 3(a)–3(c) exhibit, respectively, the behavior of the central unshifted line and of the first and second plasma satellites as a function of the D_2 gas filling pressure. It clearly shows the resonant behavior of the electron and ion waves near the theoretical resonance pressure (1.65 Torr at 23°C). *All these lines disappear when we use only one laser frequency or when the initial pressure is too low.*

By comparison with the thermal scattering level which can be calculated from the temperature and density [14], we can estimate a minimum scattered intensity measured at 10° for the electron waves at $\delta\omega$ and the ion waves of $I_s/I_0 \geq 5 \times 10^{-9} - 5 \times 10^{-8}$ and $I_s/I_0 \geq 6 \times 10^{-8} - 6 \times 10^{-7}$, respectively. The classical Bragg formula relates the scattered intensity I_s to the probe beam intensity I_0 :

$$\frac{I_s}{I_0} = \left[\frac{\pi}{2} \frac{\delta n}{n_0} \frac{n_0}{n_c} \frac{L}{\lambda} \right]^2,$$

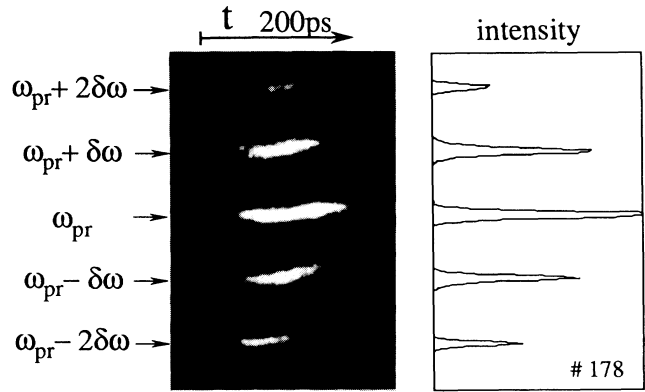


FIG. 2. A scattered spectrum measured at 10° in D_2 , 1.95 Torr, $I_{\text{max}}(\text{YAG}) = I_{\text{max}}(\text{YLF}) = 10^{14}$ W/cm^2 . The central line (ω_{probe}) is attenuated by 100 and the first satellites ($\omega_{\text{pr}} \pm \delta\omega$) by 10. Lineouts at the maximum of the emission are shown on the right.

where $\delta n/n_0$ is the relative amplitude of the density perturbation, n_c is the critical density associated with the probe beam wavelength λ , and L is the length of the plasma in the direction of observation. For a probe beam diameter of $40 \mu\text{m}$ it gives $L = 230 \mu\text{m}$ and the corresponding relative density perturbations $(\delta n/n_0)_{10^\circ} \geq (0.4 - 1.2)\%$ for the electrons and $(\delta n/n_0)_{10^\circ} \geq (1.2 - 3.7)\%$ for the ions.

Assuming that the second satellite ($2\delta\omega, \mathbf{k}_{10^\circ}$) is produced by the coupling of the detected fundamental ($\delta\omega, \mathbf{k}_{10^\circ}$) with the primary beat-generated plasma waves, the ratio R between the amplitudes of the first two satellites leads to an estimation of the amplitude of the relativistic plasma wave. From fluid equations, we first obtain the general formula for the density perturbation $n_2(2\delta\omega, \mathbf{k})$ due to the nonlinear coupling between pairs of electron waves (ω_a, \mathbf{k}_a) and (ω_b, \mathbf{k}_b) satisfying $\omega_a \approx \omega_b \approx \delta\omega$ and $\mathbf{k} = \mathbf{k}_a + \mathbf{k}_b$:

$$\frac{n_2(2\delta\omega, \mathbf{k})}{n_0} = \frac{1}{2} \sum_{\mathbf{k}_a, \mathbf{k}_b} \frac{n_{1a} n_{1b}}{n_0^2} f(\mathbf{k}_a, \mathbf{k}_b) \delta(\mathbf{k} - \mathbf{k}_a - \mathbf{k}_b), \quad (1)$$

where n_{1a} and n_{1b} represent the density perturbations of

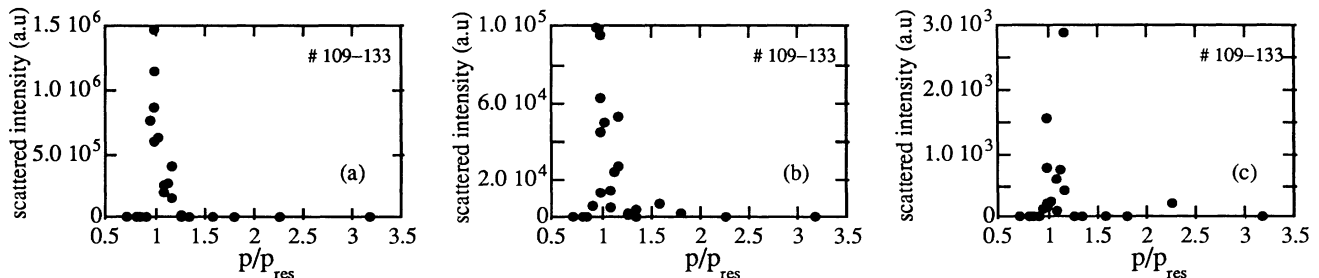


FIG. 3. Intensity at 10° as function of normalized fill pressure p/p_{res} . p_{res} is the theoretical resonance pressure (1.65 Torr). (a) Central line (ω_{pr}); (b) first satellite ($\omega_{\text{pr}} + \delta\omega$); (c) second satellite ($\omega_{\text{pr}} + 2\delta\omega$). The three vertical scales use the same unit. The points on the x axis are, respectively, 5, 4, and 2 orders of magnitude lower than the maximum signal.

the waves, $\delta=1$ when $\mathbf{k}=\mathbf{k}_a+\mathbf{k}_b$ and 0 otherwise, and

$$f(\mathbf{k}_a, \mathbf{k}_b) = \frac{1}{6} \frac{(\mathbf{k}_a + \mathbf{k}_b) \cdot [(\mathbf{k}_a \cdot \mathbf{k}_b)(\mathbf{k}_a + \mathbf{k}_b) + 2k_a^2 \mathbf{k}_b + 2k_b^2 \mathbf{k}_a]}{k_a^2 k_b^2} \quad (2)$$

Let us remark that the second satellite cannot be the second harmonic of a beat-generated plasma wave of wave vector \mathbf{k}_b for two reasons: The angle θ between \mathbf{k}_b and the laser axis is limited to $\theta_{\max}=83^\circ$ and the corresponding maximum wave vector modulus is $0.26k_{10^\circ}$, so that we can never obtain $2\mathbf{k}_b=\mathbf{k}_{10^\circ}$. Thus, we assume that the main contribution comes from the coupling of waves \mathbf{k}_b directly generated by the beat wave—which should be the most intense waves in the plasma—and waves \mathbf{k}_a generated by modulational instability (cf. Fig. 4), and we neglect the contribution of the coupling of pairs of waves generated by MI.

As k_b is small compared to k_{10° , we have $\mathbf{k}_a=\mathbf{k}_{10^\circ}-\mathbf{k}_b \approx \mathbf{k}_{10^\circ}$ and $n_{1a} \approx n_1(\delta\omega, \mathbf{k}_{10^\circ})$ which we directly measure at 10° . Each couple $\mathbf{k}_a, \mathbf{k}_b$ appears twice in [1] so that we can write for a given \mathbf{k}_b

$$\sqrt{R} = \left| \frac{n_2(2\delta\omega, \mathbf{k}_{10^\circ})}{n_1(\delta\omega, \mathbf{k}_{10^\circ})} \right| \approx \frac{|n_1(\delta\omega, \mathbf{k}_b)|}{n_0} |f(\mathbf{k}_{10^\circ} - \mathbf{k}_b, \mathbf{k}_b)|.$$

For the on-axis relativistic wave, $f=-1.28$, whereas for the wave at 83° , $f=2.62$. Now assuming a broad \mathbf{k}_b spectrum generated by the beat wave with an arbitrary but realistic amplitude dependence with θ proportional to $1-\theta^2/\theta_{\max}^2$, we get $\langle f \rangle = -0.8$ and $\langle f^2 \rangle^{1/2} = 4.4$. The first average value is relevant to the case of a completely coherent spectrum—i.e., all waves in phase—whereas the second average value is applicable to the case of uncorre-

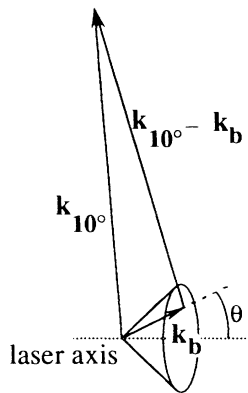


FIG. 4. Principle of the wave-coupling geometry between a beat-wave-generated plasma wave \mathbf{k}_b limited in a cone of maximum angle 83° and a plasma wave $\mathbf{k}_{10^\circ} - \mathbf{k}_b$ to produce a wave k_{10° measured on the 10° diagnostic. The maximum ratio is $k_b/k_{10^\circ}=0.26$. The scales have been modified for clarity.

lated waves. To get an *underestimate* of the beat-wave-generated density perturbation we take the *maximum* of these coupling factors. For the measured amplitude ratios $R=2 \times 10^{-3}$ to 5×10^{-2} , we obtain $n_1(\delta\omega, \mathbf{k}_b)=1\%$ to 5% . We must emphasize that this gives a local estimate of the value of the electric field independent of the assumptions made on the actual volume filled by the plasma waves.

At 0° the signal at the frequency of the probe beam is blocked in the spectrometer so that the electron satellites at $\pm \delta\omega$ are detected and the ion feature is suppressed. The intensity of the first satellite as a function of pressure does not show a clear resonance. However, an important point is that we do observe some satellites even at pressure below the resonant pressure. Null shots in vacuum do not produce these satellites, meaning that the signal is generated in the neutral gas surrounding the plasma. The third-order nonlinear susceptibility $\chi^{(3)}$ of the gas couples together the two laser beams and the probe beam [15]. A signal is therefore generated in the volume of gas common to the three beams and, having the same frequency, can hide the signal from the plasma wave. For the points near the resonance we get an upper bound of the intensity scattered by the relativistic plasma wave of the order of $I_s/I_0 \approx 10^{-5}-10^{-7}$. This gives an upper bound of $(\delta n/n_0)L$, the product of the amplitude of the plasma wave by its length, of $(0.4-4)\%$ mm. This assumes moreover that the plasma wave is coherent over the whole scattering length. We must emphasize that the absence of observed resonance at 0° is mainly due to an experimental problem with the diagnostic and is not in contradiction with the 10° results.

The signals observed at 30° correspond to a classical thermal Thomson scattering. This shows that because of Landau damping no electron waves or ion waves are generated with the corresponding wave vector.

The coherent interpretation of all these results is the following. In a first step relativistic plasma waves are generated by the beating of the two infrared laser beams. As their amplitude increases these waves become unstable with respect to MI. A whole spectrum of waves is then amplified from the thermal noise and we measure those propagating at 95° on the 10° diagnostic. A theoretical estimate has been made of the saturation level of the relativistic plasma wave due to MI. Assuming a homogeneous initial density we calculate with the use of usual fluid equations the growth of the relativistic plasma wave. At each time step we compute the growth rate of the MI [3] and assume that the wave saturates when the time integral of the growth rate reaches a value of 5 as suggested by particle simulations [3]. At this value for our experimental conditions the saturation value of $\delta n/n_0=1.5\%$ is reached 50 ps before the maximum of the laser pulses. For comparison, we note that in the absence of MI, the saturation due to relativistic detuning [2] would lead to a maximum value of 14% near the maximum of

the pulses.

In conclusion, we have observed intense ion and electron waves due to the decomposition, via modulational instability, of beat-wave-generated electron plasma waves near the resonant density. Although the amplitude of the relativistic plasma wave has not been measured directly, we have estimated it from the amplitude ratio between satellites observed at 10° . This experimental estimate of the density perturbation (1% to 5%) is in agreement with simple theoretical predictions of the maximum amplitude of the plasma waves generated by a beat wave in the presence of modulational instability (1.5%).

We gratefully acknowledge the help of all the laser and technical staff of LULI during these experiments. We are particularly grateful to B. Montes and P. Poilleux for their help in designing and running this experiment. We would also like to thank A. Dangor, A. Dyson, A. Dymoke-Bradshaw, and C. Gouédard for useful discussions. Laboratoire d'Utilisation des Lasers Intenses, Laboratoire de Physiques des Gaz et des Plasmas, Laboratoire de Physique Nucléaire des Hautes Energies, Groupe de Recherche sur l'Energétique des Milieux Ionisés, and Centre de Physique Théorique are Laboratoires associés au CNRS.

-
- [1] J. M. Dawson, *Sci. Am.* **260**, 34 (1989); *Advanced Accelerator Concepts*, edited by C. Joshi, AIP Conf. Proc. No. 193 (AIP, New York, 1989).
 [2] M. Rosenbluth and C. S. Liu, *Phys. Rev. Lett.* **29**, 701 (1972); T. Tajima and J. M. Dawson, *Phys. Rev. Lett.* **43**,

- 267 (1979); T. Katsouleas and J. M. Dawson, *Phys. Rev. Lett.* **51**, 392 (1983); P. Sprangle, E. Esarey, A. Ting, and G. Joyce, *Appl. Phys. Lett.* **53**, 2146 (1989).
 [3] P. Mora, D. Pesme, A. Héron, G. Laval, and N. Silvestre, *Phys. Rev. Lett.* **61**, 1611 (1988); D. Pesme, S. J. Kartuneeen, R. R. E. Salomaa, G. Laval, and N. Silvestre, *Laser Part. Beams* **6**, 199 (1988).
 [4] C. E. Clayton, C. Joshi, C. Darrow, and D. Umstadter, *Phys. Rev. Lett.* **54**, 2343 (1985); F. Martin and T. W. Johnston, *Phys. Rev. Lett.* **55**, 1651 (1985).
 [5] C. Darrow *et al.*, *Phys. Rev. Lett.* **56**, 2629 (1986).
 [6] N. A. Ebrahim *et al.*, SLAC Report No. 303, 1986 (available from the National Technical Information Service, U.S. Department of Commerce, 5285 Port Royal Road, Springfield, VA 22161).
 [7] F. Martin, J. P. Matte, H. Pepin, and N. A. Ebrahim, *New Developments in Particle Acceleration Techniques (Orsay, 1987)*, CERN 87-11 (available from CERN Service d'Information Scientifique, Geneva, Switzerland).
 [8] Y. Kitagawa *et al.*, in *Nonlinear Dynamics and Particle Acceleration*, edited by Y. H. Ichikawa and T. Tajima, AIP Conf. Proc. No. 230 (AIP, New York, 1991), p. 67.
 [9] A. E. Dangor, A. K. L. Dymoke-Bradshaw, and A. E. Dyson, *Phys. Scr.* **T30**, 107 (1990).
 [10] A. E. Dyson, A. E. Dangor, and A. K. L. Dymoke-Bradshaw, *J. Phys. B* **22**, L231 (1989).
 [11] A. E. Dangor, A. K. L. Dymoke-Bradshaw, and A. E. Dyson, *J. Appl. Phys.* **64**, 6182 (1988).
 [12] F. Amiranoff *et al.*, *Rev. Sci. Instrum.* **61**, 2133 (1990).
 [13] J. R. Marquès *et al.* (to be published).
 [14] J. Sheffield, *Plasma Scattering of Electromagnetic Radiation* (Academic, New York, 1975).
 [15] H. J. Lehmeier, W. Leupacher, and A. Penzkofer, *Opt. Commun.* **56**, 67 (1985).

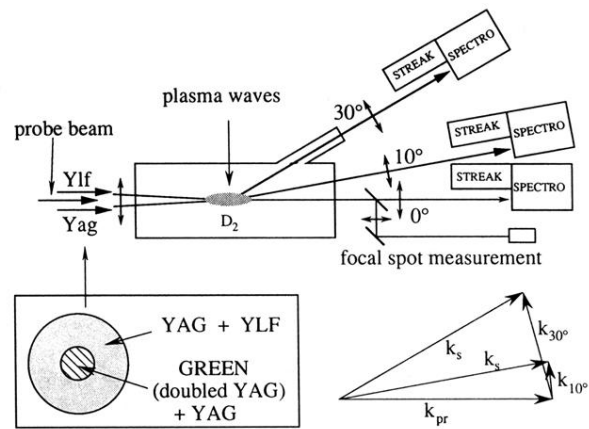


FIG. 1. Experimental setup. The three wavelengths (YAG, YLF, and doubled YAG) are spatially distributed as shown and focused in the middle of the gas chamber. k_{pr} , k_{10° , and k_{30° are the wave vectors of the probe beam and those measured at 10° and 30° . k_0 is on the axis and $\approx k_{pr}/191$.

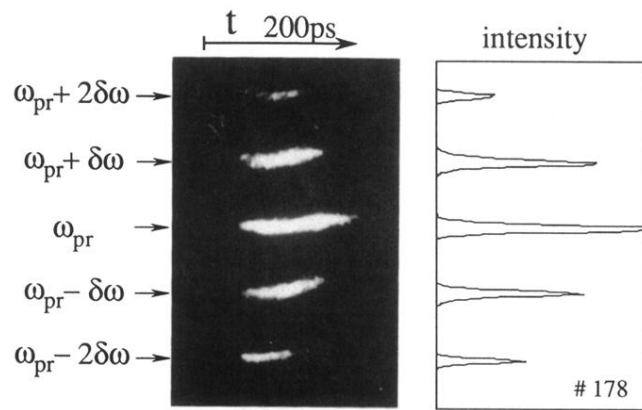


FIG. 2. A scattered spectrum measured at 10° in D_2 , 1.95 Torr, $I_{\max}(\text{YAG}) = I_{\max}(\text{YLF}) = 10^{14}$ W/cm 2 . The central line (ω_{probe}) is attenuated by 100 and the first satellites ($\omega_{\text{pr}} \pm \delta\omega$) by 10. Lineouts at the maximum of the emission are shown on the right.